# Optical Spin Injection and Spin Lifetime in Ge Heterostructures

F. Pezzoli,[1,*] F. Bottegoni,[2] D. Trivedi,[3] F. Ciccacci,[2] A. Giorgioni,[1] P. Li,[4] S. Cecchi,[2] E. Grilli,[1] Y. Song,[3] M. Guzzi,[1] H. Dery,[3,4] and G. Isella[2]

[1]*LNESS–Dipartimento di Scienza dei Materiali, Università degli Studi di Milano-Bicocca, I-20125 Milano, Italy*
[2]*LNESS–Dipartimento di Fisica, Politecnico di Milano, I-20133 Milano, Italy*
[3]*Department of Physics and Astronomy, University of Rochester, Rochester, New York 14627, USA*
[4]*Department of Electrical and Computer Engineering, University of Rochester, Rochester, New York 14627, USA*

(Received 29 June 2011; revised manuscript received 15 November 2011; published 13 April 2012)

We demonstrate optical orientation in Ge/SiGe quantum wells and study their spin properties. The ultrafast electron transfer from the center of the Brillouin zone to its edge allows us to achieve high spin polarizations and to resolve the spin dynamics of holes and electrons. The circular polarization degree of the direct gap photoluminescence exceeds the theoretical bulk limit, yielding ~37% and ~85% for transitions with heavy and light holes states, respectively. The spin lifetime of holes at the top of the valence band is estimated to be ~0.5 ps and it is governed by transitions between light and heavy hole states. Electrons at the bottom of the conduction band, on the other hand, have a spin lifetime that exceeds 5 ns below 150 K. Theoretical analysis of the spin relaxation indicates that phonon-induced intervalley scattering dictates the spin lifetime of electrons.

DOI: 10.1103/PhysRevLett.108.156603 PACS numbers: 72.25.Fe, 72.25.Rb, 78.55.−m, 78.67.De

Using the electron spin degree of freedom in semiconductors is an attractive approach to process classical or quantum information in a scalable solid state framework [1–5]. Group IV compounds have a great potential in this field because of their long spin lifetime [6–9] and the ability to suppress hyperfine interactions by purifying their zero-spin nuclear isotopes [1,4]. Despite such advantages, our understanding of spin phenomena in these materials is still at an early stage and hampered by experimental difficulties. For instance, measured spin lifetimes in electrically injected Si and Ge are strongly suppressed by interfacial effects [10–16].

In this Letter we study spin properties of holes and electrons in Ge quantum wells (QWs). By measuring the circular polarization of different photoluminescence (PL) spectral peaks we quantify the spin polarization and relaxation of optically oriented holes and electrons. The undoped and strained QWs exhibit a highly efficient spin polarization degree, yielding about 37% and 85% circularly polarized PL for direct gap transitions involving heavy and light hole states, respectively. The spin lifetime of electrons is estimated to be in the 5 ns range at 150 K and in the 0.5 ps range for holes. Our theoretical analysis shows that the spin relaxation of electrons is governed by intervalley scattering due to electron-phonon interaction. We also provide concise selection rules for the dominant phonon-assisted optical transitions. These selection rules establish a direct relation between the spin polarization of electrons and the measured circular polarization degrees of phonon-assisted transitions [17–20].

The sample investigated in this work is a type-I $Ge/Si_{0.15}Ge_{0.85}$ multiple quantum well (MQW) heterostructure deposited by low-energy plasma-enhanced CVD on a strain relaxed $Si_{0.1}Ge_{0.9}/Si(001)$ graded buffer layer [21]. The active region consists of 100 periods of a 5 nm wide Ge QW and a 10 nm thick $Si_{0.15}Ge_{0.85}$ barrier [22]. Figure 1(a) shows the calculated energy levels of its confined states using an 8-band $\mathbf{k}\cdot\mathbf{p}$ model [23,24]. Before presenting and analyzing the experimental results, we explain in the next two paragraphs the rich spin physics that one can probe by measuring the circular polarization degree of the PL in this structure. We use Fig. 1(b) to illustrate the physical processes taking place in our experimental conditions.

The investigated structure allows us to identify the dominant spin-relaxation mechanism of holes with the net transfer of photoexcited carriers from light hole to heavy hole bands. This transfer is enabled by the confinement and biaxial compressive strain which split the top of the valence band in the QW region [see Fig. 1]. In parallel with this process, photoexcited electrons are scattered from the $\Gamma$ to $L$ valley on a subpicosecond time scale [25–27]. This short dwell time in the $\Gamma$ valley renders the direct gap PL a useful tool in studying the spin lifetime of holes [28]. We will show how the spin relaxation of holes in Ge QWs can be evaluated from the measured circular polarization degrees of direct gap optical transitions involving light and heavy holes.

The lifetime of electrons in the $L$ valleys is governed by recombination processes. The energy proximity to the $\Gamma$ valley and the ultrafast transfer from it are key features in keeping the photoexcited electrons spin-polarized when reaching the $L$ valleys ($\Delta_{\Gamma\text{-}L} \sim 140$ meV in bulk Ge). Measuring a nonvanishing circular polarization from the $L$ valley luminescence is possible only if $\tau_s \gtrsim \tau_L$ where $\tau_s$ is the spin lifetime of electrons and $\tau_L$ is the indirect gap

 

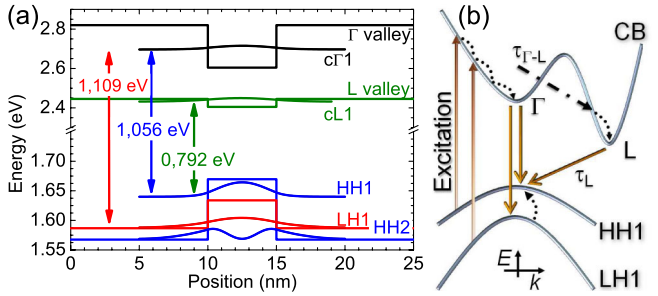


FIG. 1 (color online). (a) 8-band $\mathbf{k}\cdot\mathbf{p}$ calculation of energy levels and wave function square amplitudes for a $Si_{0.15}Ge_{0.85}/Ge/Si_{0.15}Ge_{0.85}$ quantum well. (b) Sketch of the luminescence process. Immediately after direct gap excitation, electrons can thermalize towards the edge of the Γ valley and recombine radiatively. For Γ valley electrons, however, the most effective process is scattering to the low-energy $L$ valleys, where they can recombine after $\tau_L$. The ultrafast time scale $\tau_{\Gamma\text{-}L} < 1$ ps sets the lifetime for electrons at Γ.

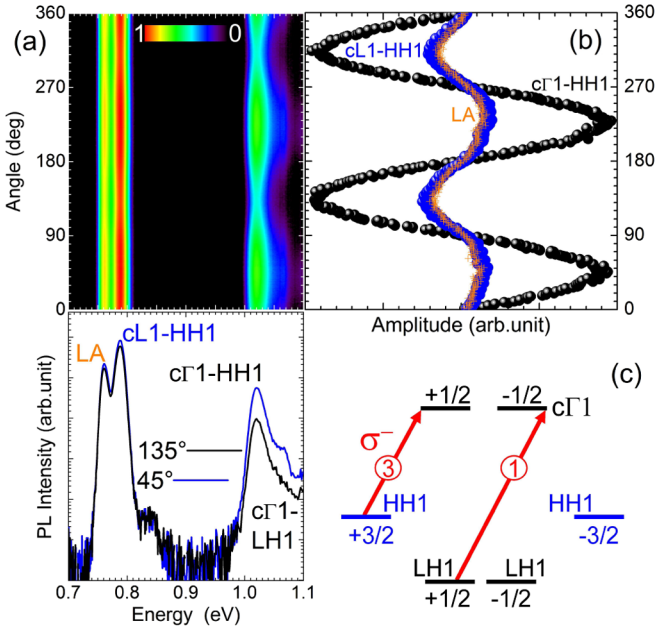


FIG. 2 (color online). (a) Color-coded contour plot of the photoluminescence intensity recorded for analyzer angles ranging from 0° to 360° for the $Ge/Si_{0.15}Ge_{0.85}$ MQW sample at 4 K and under left-handed ($\sigma^-$) circularly polarized excitation at 1.165 eV. The black and blue lines at the lower left panel refer to spectra resolved for analyzer angles of 135° and 45°, respectively. Their intensity difference at the lower energy spectral region (< 0.8 eV) stems from spin polarization of electrons, and at higher energies (> 1 eV) from spin polarization of both electrons and holes. (b) Peak amplitude modulations of the $c\Gamma1$-$HH1$, $cL1$-$HH1$ and phonon replica emissions. (c) Optical selection rules of the $\sigma^-$ excitation. Dipole allowed transitions of heavy holes ($m_j = 3/2$) are 3 times larger than of light holes ($m_j = 1/2$). Their energy levels are split by confinement and strain.

recombination lifetime (due to radiative and nonradiative channels). We will demonstrate a wide temperature range at which this condition is met in type-I Ge QWs where $\tau_L$ is of the order of a few ns [29]. This property is a clear advantage over *undoped* bulk IV semiconductors and common type-II SiGe heterostructures where the recombination lifetimes are hundreds of ns and longer [30,31].

PL measurements were performed in a backscattering geometry in a closed-cycle cryostat. A continuous wave Nd-$YVO_4$ laser, operating at 1.165 eV, was coupled to an optical retarder as circularly polarized excitation source. The laser beam was focused to a spot size having a ~100 $\mu$m diameter, resulting in an excitation density in the range of $9 \times 10^2$–$3 \times 10^3$ W/cm$^2$. PL polarization was then probed by a continuous rotation of a quarter-wave plate followed by a polarizer, long pass filters, and a grating spectrometer equipped with an InGaAs array detector [32]. Figure 2(a) shows a contour plot of the PL intensity at 4 K following $\sigma^-$ excitation as a function of the rotation angle of the polarization analyzer. The lower panel shows the resulting PL spectrum. When changing the excitation from $\sigma^-$ to $\sigma^+$ the PL spectrum remains the same but with opposite circular polarization [32].

The emission peaks in Fig. 2(a) can be rationalized by $\mathbf{k}\cdot\mathbf{p}$ [Fig. 1(a)] or tight-binding calculations [22]. The spectral feature around ~1.03 eV is due to the $c\Gamma1$-$HH1$ transition and the feature at ~1.06 eV is attributed to the $c\Gamma1$-$LH1$ excitonic recombination. The latter is superimposed onto the broad high energy tail of the main $c\Gamma1$-$HH1$ peak. The low-energy PL doublet, at ~0.8 eV, is associated with transitions across the indirect band gap: the high energy part is ascribed to the no-phonon emission associated with the $cL1$-$HH1$ recombination of confined carriers, while the low-energy part of the doublet is the longitudinal acoustic (LA) phonon-assisted optical transition [22]. Figure 2(b) shows the amplitude modulation of the PL peaks for the $c\Gamma1$-$HH1$ (black dots), $cL1$-$HH1$ (blue dots), and the phonon replica (orange crosses) transitions. This figure reveals a sinusoidal behavior with period $\pi$, characteristic of circularly polarized emission with the same helicity of the excitation. Such observation is indeed corroborated by a full polarimetric analysis based on the measurement of Stokes parameters [32].

The polarization analysis of the direct gap emission [> 1 eV in Fig. 2(a)] sheds light on the spin-relaxation of holes. Under $\sigma^-$ excitation at 1.165 eV, electrons are injected to $|J, J_z\rangle = |1/2, 1/2\rangle$ conduction states starting from $|3/2, 3/2\rangle$ heavy hole states, as well as to $|1/2, -1/2\rangle$ conduction states starting from $|3/2, 1/2\rangle$ light hole states [Fig. 2(c)]. According to tight-binding calculations [18] and data available for III-V QWs [33], the overall electron polarization right after injection is expected to be $P_0 \approx$ 28%–34% for excitation away from the first confined $HH$ and $LH$ states. Under the assumption of complete heavy holes depolarization and after thermalization towards the $c\Gamma1$ level, electrons can recombine with either $|3/2, 3/2\rangle$

or $|3/2, -3/2\rangle$ holes emitting, respectively, $\sigma^-$ or $\sigma^+$ circularly polarized light. Assuming electron spin depolarization to be negligible, the luminescence circular polarization degree for the $c\Gamma 1$-$HH1$ transition is $P_c \approx 0.96 P_0$ [18]. The consistency of this conclusion with our experimental finding of 37% ±5% validates the presence of equal numbers of heavy holes in the two sublevels, despite the fact that only $|3/2, +3/2\rangle$ holes are created upon $\sigma^-$ excitation [Fig. 2(c)]. Most importantly, the mechanisms leading to equalization of the $|3/2, -3/2\rangle$ and $|3/2, 3/2\rangle$ populations take place on a time scale faster than that of the electron scattering to $L$ valleys ($\tau_{\Gamma\text{-}L} \approx 0.5$ ps [26]).

To understand the depolarization of heavy holes we analyze the well-resolved feature around ~1.06 eV [$c\Gamma 1$-$LH1$ in Fig. 2(a)]. Being superimposed on the high energy tail of the $c\Gamma 1$-$HH1$ peak, we estimated its polarization degree by subtracting the exponential Boltzmann-like tail of the $HH1$ transition from the spectra obtained at analyzer angles of $\pi/4$ and $3\pi/4$ [32]. By doing so, we obtain a polarization as high as 85% ±17% at this spectral region. This large measured value indicates that photoexcited light holes ($|3/2, +1/2\rangle$) do not lose their spin orientation [34]. They either recombine with $|1/2, -1/2\rangle$ electrons or relax into lower energy $|3/2, -3/2\rangle$ heavy hole states via parity-preserving scattering events [33]. This relaxation process counterbalances (and depolarizes) the population of photoexcited heavy holes in $|3/2, 3/2\rangle$ states. The higher energy of the confined light hole band inhibits inward scattering from heavy holes and, consequently, the spin relaxation of light holes in this structure is longer. From the large measured circular polarization degree of the $c\Gamma 1$-$LH1$ transition we infer that it is longer than $\tau_{\Gamma\text{-}L}$.

We now focus on the indirect band-gap luminescence. The lower left panel of Fig. 2(a) shows the no-phonon (NP) $cL1$-$HH1$ peak at ~0.79 eV and the LA phonon-assisted peak at ~0.76 eV. In the Supplemental Material we show that the polarized component of the indirect transition at 4 K has a nearly complete $\sigma^-$ character [32]. The NP peak reveals a polarization degree of about 8% ±5%, and similarly the LA peak displays 6% ±5%. We employ group theory analysis similar to Ref. [17] and find the ratio of intensities between left and right circularly polarized PL detected after propagating along the [001] crystallographic direction. Following recombination of heavy holes with spin-down electrons from any of the four $L$ valleys, we get that $I_{\sigma^-}:I_{\sigma_+} = 3{:}1$ for the dominant LA assisted transition (25 meV below the band edge). For the weaker TO (36 meV) and TA (8 meV) assisted transitions the ratios are 1:3 and 1:0, respectively. The slight difference in measured polarizations of the NP (~ 8%) and LA replica (~ 6%) can be explained by the proximity of the weak TA transition to the NP emission region and of the weak TO transition to the LA region. Considering the aforementioned initial electron polarization of $P_0 \approx 30\%$ at the $\Gamma$ valley, and the predicted LA intensity $I^{\mathrm{LA}}_{\sigma^-}/I^{\mathrm{LA}}_{\sigma_+} = 3$ one should expect at most $P_c \approx 15\%$. We attribute the smaller measured average value (~ 6%) to two spin-relaxation mechanisms. The first is due to electron-hole exchange interaction of confined exciton states. This mechanism plays an important role at liquid-helium temperature and in intrinsic QWs [35]. The second relaxation process is attributed to the Elliott-Yafet mechanism via intervalley electron scattering by shortwave phonon modes. As explained below, this mechanism pertains to higher temperatures.

To extract the spin relaxation of electrons, we performed a Stokes analysis of both NP and LA emissions as a function of the lattice temperature [32]. Figure 3 shows that below 150 K the measured polarization of the indirect band-gap luminescence in Ge/SiGe MQWs is nearly temperature independent [36]. This observation is a clear indication that the optically oriented spins withstand the ultrafast relaxation to the $L$ valleys as well as the dwell time of electrons in the $L$ valleys before recombination. Making use of recent PL decay measurements of the recombination lifetime performed on similar samples with slightly different QW widths (3.8 and 7.3 nm) [29], we extrapolated the electron lifetime, $\tau_L$, for the NP transition in our Ge QWs. As shown by the blue curve of Fig. 3, $\tau_L$ is below 10 ns across the entire temperature range (14–300 K).

To complete the picture we have also performed spin-relaxation analysis due to electron-phonon scattering. The sharply decreasing (black) curve in Fig. 3 shows the resulting spin-relaxation time ($\tau_s$) in intrinsic Ge. Simulations were made using a spin-dependent $\mathbf{k} \cdot \mathbf{p}$ expansion at the vicinity of the $L$ point. Similar to the spin-dependent expansion near the $X$ point of silicon [37], such modeling provides useful insights. The detailed theory will be shown

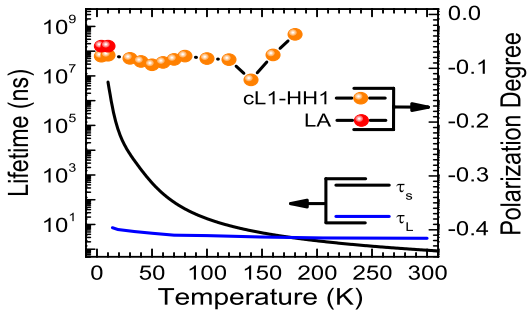


FIG. 3 (color online). Dots: Measured temperature dependence of the circular polarization degree at the peak region of the no-phonon ($cL1$-$HH1$) emission (orange dots). Results of the LA phonon-assisted emission (red dots) are shown at $T < 20$ K where it is well resolved from the $cL1$-$HH1$ peak. Black line: Modeled temperature dependence of the electron spin lifetime due to electron-phonon interaction. Blue line: Measured recombination lifetime due to radiative and nonradiative channels in a ~5 nm wide Ge/SiGe QW (after [29]).

in a different paper and here we mention key findings. Around 150 K, $\tau_s \approx 5$ ns is comparable with the recombination lifetime $\tau_L$. Taking into account the dependence of the circular polarization on these time scales, $P_c = P_c^0/(1 + \tau_L/\tau_s)$ [38], we can explain the behavior of the measured circular polarization as a function of temperature. The theory shows that spin relaxation is governed by *intervalley* electron-phonon scattering in a wide temperature range ($T > 30$ K) [39]. This dominating mechanism involves shortwave phonon modes whose wave vector connect centers of different $L$ valleys (i.e., phonon modes near the $X$ point). Dominant contributions result from the $X_4$ and $X_1$ symmetries where their phonon energies are $\approx 30$ meV. The temperature dependence of this spin-relaxation mechanism is governed by the Bose-Einstein distribution of these phonon modes. Using the symmetries of the $D_{3d}$ group at the $L$ point, the intervalley spin-relaxation rate can be shown to depend on the spin-orbit coupling between conduction bands and not between conduction and valence bands. At very low temperatures the population of $X$ point phonon modes is negligible and as a result the *intravalley* spin-relaxation rate can exceed the *intervalley* rate. The former, originally predicted by Yafet to have a $T^{7/2}$ temperature dependence [40], results in spin lifetimes of the order of a few $\mu$s or longer at low temperatures. Practically, however, such a long time scale will be easily masked by localization (freeze-out conditions), electron-hole exchange, or doping effects.

The findings of this work are important for several reasons. First, the extracted electron spin relaxation of undoped Ge QWs is comparable to bulk Ge [9], while being much longer than that in ferromagnet/oxide/Ge structures. In the latter case, it is reasonable that localized states at the interface between the tunnel barrier and the semiconductor mask the spin signal of the itinerant electrons [12–14]. Second, the extracted spin lifetime of holes is important in clarifying recent Hanle measurements in heavily-doped $p$-type silicon and germanium [10,16,41]. The ultrafast spin relaxation of holes is governed by transitions between light and heavy hole bands. The mixed spin components of light holes lead to these enhanced rates [33]. The magnitude of the spin-orbit coupling, as manifested by the energy difference from the split-off band, hardly plays a role in setting the scattering rate. Our findings of a 0.5 ps hole spin lifetime are in agreement with previous experimental results [25,42,43], and may imply that localized interfacial states rather than free holes give rise to the non-negligible spin lifetime in ferromagnet/oxide/$p$-type semiconductor structures [10]. Finally, the compatibility with the mainstream Si technology renders Ge an unmatched candidate in group IV photonics [44,45]. In the case of Ge QWs, confinement and strain allow one to tune the spectral emission, resolve contributions of different hole species, and analyze indirect optical transitions.

In conclusion, we have demonstrated efficient and robust optical spin orientation in Ge/SiGe MQWs. The photoluminescence from Ge quantum wells is shown to be an efficient tool in studying the spin lifetimes of holes and electrons. The measured circular polarization degrees suggest that after optical orientation carriers do not completely lose their spin memory when they cool down or experience intervalley scattering. These results are particularly exciting for spintronic applications, since an optical spin injection scheme based upon the $\Gamma$-to-$L$ spin transfer bypasses detrimental interfacial effects of all-electrical ferromagnet/oxide/Ge injection schemes. The efficient optical emission and spin polarization at the direct gap of Ge-based heterostructures open up a unique possibility to merge the potential of both photonics and spintronics on the well-established silicon platform.

This work was supported by the PRIN Project No. 20085JEW12, by Regione Lombardia through Dote ricercatori, by AFOSR Contract No. FA9550-09-1-0493, and by NSF Contract No. ECCS-0824075. The authors would like to thank E. Gatti and D. Chrastina for their support in sample design and preparation and A. Rastelli for the use of xrsp software.

*fabio.pezzoli@unimib.it

[1] B. E. Kane, Nature (London) **393**, 133 (1998).
[2] S. A. Wolf, D. D. Awschalom, R. A. Buhrman, J. M. Daughton, S. von Molnar, M. L. Roukes, A. Y. Chtchelkanova, and D. M. Treger, Science **294**, 1488 (2001).
[3] I. Žutić, J. Fabian, and S. Das Sarma, Rev. Mod. Phys. **76**, 323 (2004).
[4] P. S. Fodor and J. Levy, J. Phys. Condens. Matter **18**, S745 (2006).
[5] H. Dery, P. Dalal, Cywinski, and L. J. Sham, Nature (London) **447**, 573 (2007).
[6] I. Appelbaum, B. Q. Huang, and D. J. Monsma, Nature (London) **447**, 295 (2007).
[7] E.-S. Liu, J. Nah, K. M. Varahramyan, and E. Tutuc, Nano Lett. **10**, 3297 (2010).
[8] W. Han, K. Pi, K. M. McCreary, Y. Li, J. J. I. Wong, A. G. Swartz, and R. K. Kawakami, Phys. Rev. Lett. **105**, 167202 (2010).
[9] C. Guite and V. Venkataraman, Phys. Rev. Lett. **107**, 166603 (2011).
[10] H. Saito, S. Watanabe, Y. Minenob, S. Sharma, R. Jansen, S. Yuasa, and K. Ando, Solid State Commun. **151**, 1159 (2011).
[11] Y. Zhou, W. Han, L.-T. Chang, F. Xiu, M. Wang, M. Oehme, I. A. Fischer, J. Schulze, R. K. Kawakami, and K. L. Wang, Phys. Rev. B **84**, 125323 (2011).
[12] K.-R. Jeon, B.-C. Min, Y.-H. Jo, H.-S. Lee, I.-J. Shin, C.-Y. Park, S.-Y. Park, and S.-C. Shin, Phys. Rev. B **84**, 165315 (2011).
[13] A. Jain, L. Louahadj, J. Peiro, J. C. Le Breton, C. Vergnaud, A. Barski, C. Beigné, L. Notin, A. Marty,

V. Baltz, S. Auffret, E. Augendre, H. Jaffrès, J. M. George, and M. Jamet, Appl. Phys. Lett. **99**, 162102 (2011)
[14] K. Kasahara, Y. Baba, K. Yamane, Y. Ando, S. Yamada, Y. Hoshi, K. Sawano, M. Miyao, and K. Hamaya, J. Appl. Phys. **111**, 07C503 (2012).
[15] C. H. Li, O. M. J. van't Erve, and B. T. Jonker, Nature Commun. **2**, 245 (2011).
[16] S. P. Dash, S. Sharma, R. S. Patel, M. P. de Jong, and R. Jansen, Nature (London) **462**, 491 (2009).
[17] P. Li and H. Dery, Phys. Rev. Lett. **105**, 037204 (2010).
[18] M. Virgilio and G. Grosso, Phys. Rev. B **80**, 205309 (2009).
[19] J. Rioux and J. E. Sipe, Phys. Rev. B **81**, 155215 (2010).
[20] J. L. Cheng, J. Rioux, J. Fabian, and J. E. Sipe, Phys. Rev. B **83**, 165211 (2011).
[21] C. Rosenblad, H. R. Deller, A. Dommann, T. Meyer, P. Schroeter, and H. von Kanel, J. Vac. Sci. Technol. A **16**, 2785 (1998).
[22] M. Bonfanti, E. Grilli, M. Guzzi, M. Virgilio, G. Grosso, D. Chrastina, G. Isella, H. von Känel, and A. Neels, Phys. Rev. B **78**, 041407(R) (2008).
[23] http://www.nextnano.de
[24] D. J. Paul, Phys. Rev. B **77**, 155323 (2008).
[25] E. J. Loren, B. A. Ruzicka, L. K. Werake, H. Zhao, H. M. van Driel, and A. L. Smirl, Appl. Phys. Lett. **95**, 092107 (2009).
[26] C. Lange, N. S. Koster, S. Chatterjee, H. Sigg, D. Chrastina, G. Isella, H. von Känel, M. Schäfer, M. Kira, and S. W. Koch, Phys. Rev. B **79**, 201306(R) (2009).
[27] E. Gatti, E. Grilli, M. Guzzi, D. Chrastina, G. Isella, and H. von Känel, Appl. Phys. Lett. **98**, 031106 (2011).
[28] Assuming a time constant of $\tau_{\Gamma,r} \sim 1$ ns for direct gap radiative recombination, we can estimate that during the ultrashort dwell time of photoexcited electrons in the $\Gamma$ valley about $\tau_{\Gamma\text{-}L}/\tau_{\Gamma,r} \sim 10^{-3}$ of their population experience radiative recombination rather than ultrafast transfer to $L$ valleys.
[29] A. Giorgioni, E. Gatti, E. Grilli, A. Chernikov, S. Chatterjee, D. Chrastina, G. Isella, and M. Guzzi, J. Appl. Phys. **111**, 013501 (2012).
[30] J. C. Sturm, H. Manoharan, L. C. Lenchyshyn, M. L. W. Thewalt, N. L. Rowell, J.-P. Noël, and D. C. Houghton, Phys. Rev. Lett. **66**, 1362 (1991).
[31] J. Pankove, *Optical Processes in Semiconductors* (Dover, New York, 1971), Chap. 6.
[32] See Supplemental Material at http://link.aps.org/supplemental/10.1103/PhysRevLett.108.156603 for technical details of the experiment and the polarimetric analysis.
[33] T. Uenoyama and L. J. Sham, Phys. Rev. Lett. **64**, 3070 (1990).
[34] Since the weak $c\Gamma 1$-$LH1$ $\sigma^+$ emission is related only to $|1/2, +1/2\rangle$ electrons recombining with $|3/2, -1/2\rangle$ light holes, we conclude that mostly $|3/2, +1/2\rangle$ are present in the sample.
[35] M. Z. Maialle, E. A. de Andrada e Silva, and L. J. Sham, Phys. Rev. B **47**, 15 776 (1993).
[36] By increasing the temperature the band gap shrinks and above 150 K the indirect gap emission starts to leak out of the spectral range of our apparatus.
[37] P. Li and H. Dery, Phys. Rev. Lett. **107**, 107203 (2011).
[38] R. R. Parsons, Phys. Rev. Lett. **23**, 1152 (1969).
[39] J.-M. Tang, B. T. Collins, and M. E. Flatte, Phys. Rev. B **85**, 045202 (2012).
[40] Y. Yafet, *Solid State Physics*, edited by F. Seitz and D. Turnbull (Academic, New York, 1963), Vol. 14, p. 1.
[41] N. W. Gray and A. Tiwari, Appl. Phys. Lett. **98**, 102112 (2011).
[42] D. J. Hilton and C. L. Tang, Phys. Rev. Lett. **89**, 146601 (2002).
[43] E. J. Loren, J. Rioux, C. Lange, J. E. Sipe, H. M. van Driel, and A. L. Smirl, Phys. Rev. B **84**, 214307 (2011).
[44] J. Michel, J. F. Liu, and L. C. Kimerling, Nature Photon. **4**, 527 (2010).
[45] R. Soref, Nature Photon. **4**, 495 (2010).